Magnetite Nanoparticle Dispersions Stabilized with Triblock Copolymers

L. A. Harris,[†,§] J. D. Goff,[†] A. Y. Carmichael,[†] J. S. Riffle,*[,†] J. J. Harburn,[‡] T. G. St. Pierre,[§] and M. Saunders[||]

Department of Chemistry, Virginia Tech, Blacksburg, Virginia 24061, Stereotaxis Inc., St. Louis, Missouri 63108, and School of Physics and Centre for Microscopy & Microanalysis, The University of Western Australia, Crawley, Western Australia 6009, Australia

Received October 8, 2002. Revised Manuscript Received January 15, 2003

Magnetic nanoparticles that display high saturation magnetization and high magnetic susceptibility are of great interest for medical applications. Magnetite nanoparticles display strong ferrimagnetic behavior and are less sensitive to oxidation than magnetic transition metal nanoparticles such as cobalt, iron, and nickel. For in vivo applications, well-defined organic coatings are needed to surround the magnetite nanoparticles and prevent any aggregation. The goal of this research was to develop complexes of magnetite nanoparticles coated with well-defined hydrophilic polymers so that they could be dispersed in aqueous fluids. Focal points have included the following: (1) Investigations of polymer systems that bind irreversibly to magnetite at the physiological pH, (2) the design of block copolymers with anchor and tail blocks to enable dispersion in biological fluids, and (3) investigations of copolymer block lengths to maximize the concentration of bound magnetite. Hydrophilic triblock copolymers with controlled concentrations of pendent carboxylic acid binding groups were designed as steric stabilizers for magnetite nanoparticles. These copolymers were comprised of controlled molecular weight poly(ethylene oxide) tail blocks and a central, polyurethane anchor block containing carboxylic acids. Stoichiometric aqueous solutions of $FeCl_2$ and $FeCl_3$ were condensed by reaction with NH_4OH to form magnetite nanoparticles, and then a dichloromethane solution of the block copolymer was added to adsorb the copolymer onto the magnetite surfaces. Stable magnetite dispersions were prepared with all of the triblock copolymers. The polymer−nanomagnetite conjugates described in this paper had a maximum saturation magnetization of 34 emu/g. Magnetization curves showed minimal hysteresis. Powder X-ray diffraction (XRD), selected area electron diffraction (SAED), and high-resolution electron microscopy (HREM) confirmed the magnetite crystal structure. Transmission electron microscopy (TEM) showed that the dispersions contained magnetite particles coated with the polymers with a mean diameter of 8.8 ± S.D. 2.7 nm.

I. Introduction

Magnetic nanoparticles display magnetic properties different from their bulk material counterparts. These unique properties originate from the size of the particles, which are below a critical diameter for magnetic domain wall formation. In the absence of an externally applied magnetic field, thermal energy can be sufficient to cause the magnetic moments in these single-domain particles to equilibrate and overcome any preferential orientation. However, when the particles are placed in an external magnetic field, their magnetic moments align rapidly in the direction of the field and the materials display a net magnetization. When the magnetic field is removed, thermal energy is again sufficient to cause the particles' vector moments to fluctuate randomly. The magnetization of the magnetite nanoparticles investigated in this work disappears when the external field is removed (i.e., they have near zero magnetic remanence and coercivity) in short times relative to the experiment time. These properties indicate superparamagnetic behavior, which suggests that the nanoparticles may be ideal components of vehicles for magnetic field-directed delivery of therapeutic agents.

Magnetic nanoparticles can be dispersed in carrier fluids through specific interactions between the particle surfaces and selected low molecular weight or polymeric surfactants. Such fluid dispersions of small magnetic particles are known as "ferrofluids".[1] Magnetic attractive forces combined with inherently large surface energies (>100 dyn/cm)[2] favor nanoparticle aggregation in magnetic dispersions.[1,3] Thus, the properties of the surfactants and the nature and concentration of binding sites between surfactants and the particle surface are

* To whom correspondence should be addressed.
[†] Virginia Tech.
[‡] Stereotaxis Inc.
[§] School of Physics, The University of Western Australia.
[||] Centre for Microscopy & Microanalysis, The University of Western Australia.

(1) Rosensweig, R. E. *Ferrohydrodynamics*; Cambridge University Press: Cambridge, 1985.
(2) Kim, D. K.; Zhang, Y.; Voit, W.; Rao, K. V.; Muhammed, M. *J. Magn. Magn. Mater.* **2001**, *225*, 30−36.
(3) Blum, E.; Cebers, A.; Maiorov, M. M. *Magnetic Fluids*; Walter de Gruyter: Berlin, 1997.

10.1021/cm020994n CCC: $25.00
Published on Web 02/28/2003

important for defining good dispersion conditions (without particle aggregation).

Current and potential applications for magnetic nanomaterials in electronics and biotechnology are diverse. Nanomagnetic films have great promise for electronic and electrical devices, sensors, electromagnetic shielding, and high-density digital storage.[4] Biomedical applications under current investigation include retinal detachment therapy,[5] cell separation methods,[6,7] tumor hyperthermia,[8] improved MRI diagnostic contrast agents,[2,9−11] and magnetic field-guided carriers for localizing drugs or radioactive therapies.[12−14]

The nanoparticle surface can influence material durability in biological environments and also biocompatibility. These particles must remain nonaggregated, be stable against oxidation, and display high magnetization during application. Transition metals offer high magnetization, but are sensitive to oxidation. This results in loss of magnetic response owing to the formation of antiferromagnetic oxides. Currently, oxidization of the transition metals remains a hurdle, especially in biomedical, oxygen-rich environments. Iron oxides, such as magnetite (Fe_3O_4) and maghemite (γ-Fe_2O_3), are more stable against oxidation. These materials can be formed at low temperatures under mild conditions and display strong ferrimagnetic behavior. In addition, previous investigations have shown that magnetite has high LD_{50} values (LD_{50} in rats = 400 mg/kg) and polymer-coated magnetite has not shown any acute or subacute toxicity in animal studies.[15]

Magnetite particles are commonly prepared by condensing divalent and trivalent iron salts in reactions with hydroxide bases (pH of 9.5−10). The magnetite crystal structure forms readily in aqueous media. Methods to prevent agglomeration include the use of electrostatic and steric (entropic) stabilizers. Aqueous dispersions have been reported using electrostatic stabilizers,[16] bilayer surfactants,[17−20] polymers as steric stabilizers,[21−26] and polymer templates.[27] Applications of the magnetite dispersions comprised of electrostatic stabilizers and bilayer surfactants are limited due to pH sensitivity and dispersion stability, respectively. It should also be noted that many of the reported stabilizers have not been designed with functional groups to bind to the magnetite surface, and thus, dispersion stability has been limited.

In this paper we report the preparation of novel, hydrophilic, triblock copolymers containing controlled concentrations of carboxylic acid groups in the central segments and poly(ethylene oxide) tails (PEO−COOH−PEO) (Figure 1). A method for preparing magnetite nanoparticles and subsequent stabilization and dispersion using these polymers is described. The resultant polymer-coated magnetite nanoparticles were 8.8 ± S.D. 2.7 nm in diameter and appeared to be single crystals. They were dispersible in both water and chlorinated organic solvents, both of which are good solvents for the poly(ethylene oxide) tail blocks. These dispersions were stable in pH ranges common for biological systems and at the isoelectric point of uncoated magnetite (pH ≈ 6.8[1]).

II. Experimental Section

Materials. Tetrahydrofuran (THF, EM Science, 99.5%) was refluxed over sodium with benzophenone until the solution was deep purple and then fractionally distilled just prior to use. Potassium *tert*-butoxide (Aldrich, 1.03 M in THF) was stored under nitrogen and used as received. Ethylene oxide (Kodak) was dried over calcium hydride, distilled onto activated 4-Å molecular sieves, and stored under N_2 at 0 °C. Glacial acetic acid (Aldrich) was diluted to a 4 M aqueous solution. Dimethylformamide (DMF, EM Science) was dried over CaH_2, fractionally distilled to a clean, dry, round-bottom flask containing activated molecular sieves (4 Å), and stored under N_2 at 25 °C. Isophorone diisocyanate (Aldrich, 99.5%) was fractionally distilled and stored under N_2. Poly(ethylene oxide) monomethyl ether oligomers (PEO), 770, 1930, and 4845 g/mol M_n, were purchased from Aldrich. A 16 470 g/mol M_n poly(ethylene oxide) mono-*tert*-butyl ether was synthesized by anionic living polymerization of ethylene oxide monomer in a high-pressure Series 4561 Parr reactor. All monofunctional PEO oligomers were dried overnight at 80 °C under reduced pressure prior to their incorporation into triblock copolymers. Bis(hydroxymethyl)propionic acid (Aldrich) was dried in a vacuum oven at 60 °C for 2 days prior to use. Dibutyltin dilaurate (DBTL, Aldrich) catalyst was used as received.

$FeCl_3 \cdot 6H_2O$ and $FeCl_2 \cdot 4H_2O$ (Aldrich) were stored under N_2 in a desiccator and used without further purification. All water used was filtered with Millipore gradient A10 (specific conductance ≈0.52 μS/cm) and deoxygenated for a minimum of 30 min with ultra-high-purity N_2 (99.9+%). Ammonium hydroxide (50% v/v aqueous, Alfa-Aesar) was deoxygenated prior to use for a minimum of 30 min with ultra-high-purity N_2. Dichloromethane (Burdick and Jackson) was used as received. Hydrochloric acid (Aldrich) was diluted to a 25% v/v aqueous solution.

(4) Leslie-Pelecky, D. L.; Rieke, R. D. *Chem. Mater.* **1996**, *8*, 1770−1783.
(5) Phillips, J. P.; Li, C.; Dailey, J. P.; Riffle, J. S. *J. Magn. Magn. Mater.* **1999**, *194*, 140−148.
(6) Molday, R. S.; MacKenzie, D. *J. Immunol. Methods* **1982**, *52*, 353−367.
(7) Roath, S. *J. Magn. Magn. Mater.* **1993**, *122*, 329−334.
(8) Jordan, A.; Scholz, R.; Wust, P.; Schbirra,H.; Schiestel, T.; Schmidt, H.; Felix, R. *J. Magn. Magn. Mater.* **1999**, *194*, 185−196.
(9) Kim, D. K.; Zhang, Y.; Kehr, J.; Klason, T.; Bjelke, B.; Muhammed, M. *J. Magn. Magn. Mater.* **2001**, *225*, 256−261.
(10) Babes, L.; Denizot, B.; Tanguy, G.; Le Jeune, J. J.; Jallet, P. *J. Colloid Interface Sci.* **1999**, *212*, 474−482.
(11) Papisov, M. I.; Bogdanov, A., Jr.; Schaffer, B.; Nossiff, N.; Shen, T.; Weissleder, R.; Brady, T. J. *J. Magn. Magn. Mater.* **1993**, *122*, 383−386.
(12) Widder, K.; Flouret, G.; Senyei, A. *J. Pharm. Sci.* **1979**, *68*, 79−82.
(13) Gupta, P. K.; Hung, C. T.; Lam, F. C.; Perrier, D. G. *Int. J. Pharm.* **1988**, *43*, 167−177.
(14) Ibrahim, A.; Couvreur, P.; Roland, M.; Speiser, P. *J. Pharm. Pharmacol.* **1982**, *35*, 59−61.
(15) Iannone, A.; Magin, R. L.; Walczack, T.; Federico, M.; Swartz, H. M.; Tomasi, A.; Vannini, V. *Magn. Reson. Med.* **1991**, *22*, 435−442.
(16) Bacri, J.; Perzynski, R.; Salin, D.; Cabuil, V.; Massart, R. *J. Magn. Magn. Mater.* **1990**, *85*, 27−32.
(17) Khalafalla, S. E.; Reimers, G. W. *IEEE Trans. Magn.* **1980**, *Mag-16*, 178−183.
(18) Shen, L.; Stachowiak, A.; Hatton, T. A.; Laibinis, P. E. *Langmuir* **2000**, *16*, 9907−9911.
(19) Shen, L.; Stachowiak, A.; Seif-Eddeen, K. F.; Laibinis, P. E.; Hatton, T. A. *Langmuir* **2001**, *17*, 288−299.
(20) Shimoiizaka, J.; Nakatsuka, K.; Fujita, T.; Kounosu, A. *IEEE Trans. Magn.* **1980**, *MAG-16*, 368−371.
(21) Wormuth, K. *J. Colloid Interface Sci.* **2001**, *241*, 366−377.
(22) Pardoe, H.; Chua-anusorn, W.; St. Pierre, T. G.; Dobson, J. *J. Magn. Magn. Mater.* **2001**, *225*, 41−46.
(23) Mendenhall, G. D.; Geng, Y.; Hwang, J. *J. Colloid Interface Sci.* **1996**, *184*, 519−526.
(24) Lee, J.; Isobe, T.; Senna, M. *J. Colloid Interface Sci.* **1996**, *177*, 490−494.
(25) Palmacci, S.; Josephson, L.; Groman, E. V. *Synthesis of Polymer-Covered Superparamagnetic Oxide Colloids for Magnetic Resonance Contrast Agents or Other Applications*; PCT WO 9505669, 8/12/93.
(26) Ding, X. B.; Sun, Z. H.; Wan, G. X.; Jiang, Y. Y. *React. Funct. Polym.* **1998**, *38*, 11−15.
(27) Underhill, R. S.; Liu, G. *Chem. Mater.* **2000**, *12*, 2082−2091.

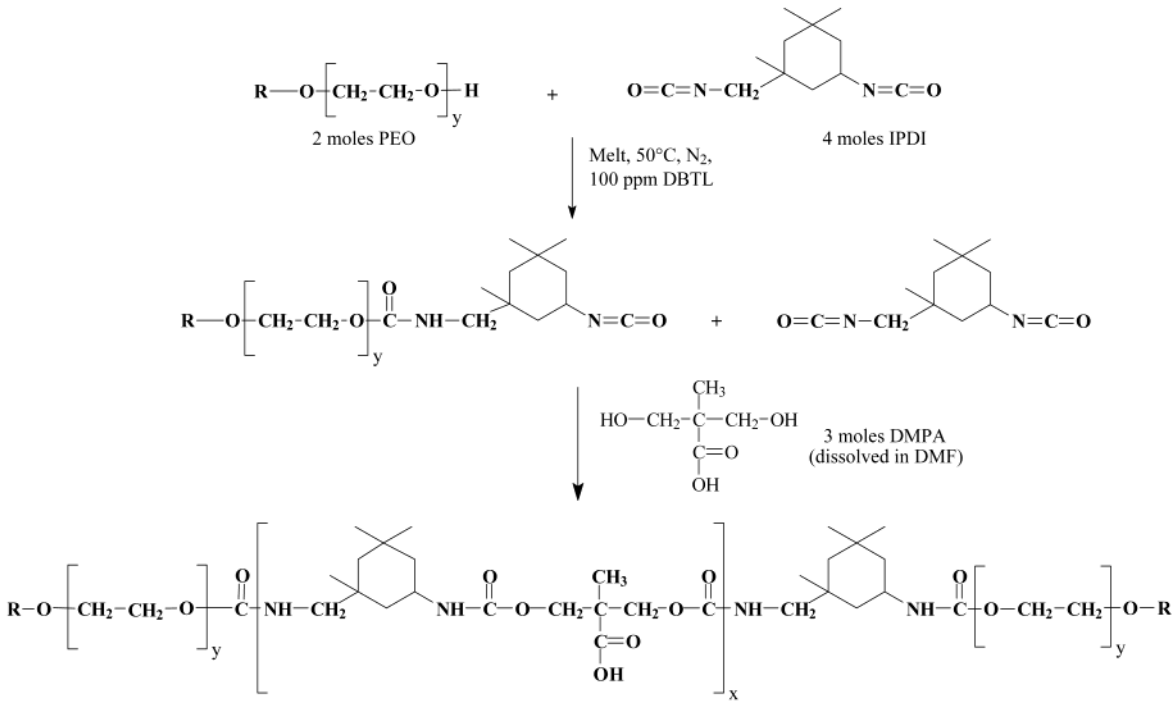

Figure 1. Controlled molecular weight triblock dispersion stabilizers comprised of hydrophilic poly(ethylene oxide) tail blocks and central, polyurethane segments containing carboxylic acid binding groups. "*x*" = ≈3−10; "*y*" = ≈17−373; R = CH_3 or *tert*-butyl.

Synthesis and Dispersion Formation. *Synthesis of a 16 470 g/mol Monofunctional Poly(ethylene oxide) Oligomer To Be Used as a Component in the Triblock Copolymer Stabilizers.* Ethylene oxide monomer (60.4 g) was transferred to the chamber of a clean, dry, 300-mL Parr reactor via a cannula using a slight pressure gradient (vacuum) toward the receiver flask, where the receiver flask was chilled externally with a dry ice/2-propanol bath. Potassium *tert*-butoxide initiator in THF (3.91 mL, 1.03 M) and 100 mL of THF solvent were syringed into the reactor with stirring. The temperature was slowly increased to 60 °C and the exotherm signifying anionic initiation of the monomer was observed with an increase in temperature (up to 131 °C) and pressure (up to 120 psi) in the Parr reactor. The polymerization was monitored by the decrease in pressure (≈10 h) at 60 °C with stirring. The living polymerization was terminated with an excess of dilute acetic acid (2.46 mL, 4 M). Upon reaction completion, the THF was removed under reduced pressure. The polymer was dissolved in hot acetone and cooled, whereupon it crystallized and precipitated. The polymer was dried in a vacuum oven at ambient temperature for 3 days.

Synthesis of Carboxylic Acid-Containing Triblock Copolymer Stabilizers. An exemplary procedure for a triblock polymer dispersion stabilizer with an average of approximately 3 carboxylic acid groups in the central segments and 1930 g/mol M_n poly(ethylene oxide) tail blocks (1930PEO−3COOH−1930PEO) is provided. Copolymers with different tail block lengths (770, 1930, 4845, and 16 470 g/mol M_n) were prepared in a similar manner by appropriately varying the molar stoichiometries to obtain controlled average concentrations of carboxylic acid groups (≈3−10 units in the central segments).

The first reaction step involved capping monofunctional PEO with isophorone diisocyanate. The dried PEO (60 g of PEO, M_n = 1930 g/mol, 0.0311 mol) was transferred molten to a warm, flame-dried, three-neck, 250-mL, round-bottom flask equipped with a mechanical stirrer and N_2 inlet. Isophorone diisocyanate (13.18 mL, 0.622 mol) was syringed into the flask, and then the flask was placed in an oil bath maintained at 50 °C under N_2. Dibutyltin dilaurate catalyst (100 ppm, 0.0083 g) was added to the reaction flask via syringe. The melt reaction was monitored by Fourier transform infrared spectroscopy (FTIR) by observing the decrease of the isocyanate absorption peak at 2260 cm^{-1}. The isocyanate capping reaction required ≈30 min under these conditions.

Once all of the poly(ethylene oxide) was capped with the diisocyanate, this material and the remaining isophorone diisocyanate were chain-extended with bis(hydroxymethyl)-propionic acid (6.258 g, 0.0467 mol) dissolved in a minimal amount of purified DMF (50 mL) and another 100 ppm increment of DBTL catalyst (0.0083 g) was added. Reaction completion was determined by the absence of the isocyanate peak in the FTIR, which required ≈36 h of total reaction time for this composition. DMF was removed under reduced pressure at ≈53 °C and ≈500 mTorr. The polymer was dissolved in chloroform, and the chloroform solution was washed three times with water to remove any unreacted bis(hydroxymethyl)-propionic acid. The copolymer was coagulated and solidified by adding the chloroform mixture into an excess of cold hexane. The polymer was recovered by filtration and dried in a vacuum oven at ambient temperature.

Magnetite Formation and Steric Stabilization. A procedure for preparing a stabilized magnetite composition using a PEO−COOH−PEO triblock copolymer with 1930 g/mol M_n PEO end blocks and an average of 3.1 carboxylic acids in the central urethane segment (1930PEO−3.1COOH−1930PEO) is provided. This composition utilizes 34.9 wt % Fe_3O_4 in the reaction. All solutions (water, base, and polymer/CH_2Cl_2) were carefully deoxygenated prior to use by purging with ultra-high-purity N_2 for a minimum of 30 min.

The first reaction of this sequence involved forming magnetite nanoparticles in anaerobic conditions at ambient temperature. Aqueous solutions of $FeCl_3 \cdot 6H_2O$ (0.389 M, 2.0 g) and $FeCl_2 \cdot 4H_2O$ (0.195 M, 0.736 g) were prepared separately under N_2 and syringed into a three-neck, 250-mL, round-bottom flask equipped with a mechanical stirrer and pH electrode connected to a pH meter. The fittings for the apparatus were attached with vacuum-tight adapters to maintain an inert nitrogen environment. Immediately after the addition of the aqueous iron salts, NH_4OH (50% v/v aqueous) was quickly syringed into the flask with stirring (≈60 rpm) until a pH of 9.5 was reached (≈10 mL). The solution quickly turned black through bluish-green rust phases, indicating the formation of magnetite. Nucleation and growth of

magnetite particles were allowed to occur for 30 min with stirring under a N_2 atmosphere.

After this, the N_2 flow was removed and the steric stabilizer solution dissolved in CH_2Cl_2 (2 g of PEO−COOH−PEO polymer in 25 mL of CH_2Cl_2) was syringed into the flask and allowed to interact with the magnetite for 30 min with stirring (pH 8.5−9). The CH_2Cl_2 was subsequently removed with a strong N_2 flow (over ≈2 h) and the polymer−magnetite nanoparticle aqueous suspension was neutralized with dilute HCl (25% v/v aqueous) to pH 6.5−7. The resultant stable dispersion was transferred to a dialysis membrane (Spectra pore 7, MWCO 1000) and was dialyzed against water for 3 days, refreshing the dialysis water twice/day. Any particle aggregates in the salt-free magnetite ferrofluids were removed by centrifuging for 30-min intervals where the sediment was discarded and the process was repeated until little to no precipitation was observed in the bottom of the centrifuge tube. This generally required centrifuging the magnetite for 3−5 intervals.

Polymer Characterization. ^{1}H and quantitative ^{13}C NMR analyses were acquired on a Varian Unity 400 NMR spectrometer operating at 400 and 100.6 MHz, respectively. For quantitative ^{13}C NMR investigations of the polymer stabilizers, 0.63 g of polymer, 2.4 mL of $CDCl_3$ or d_6-DMSO, and 52 mg of chromium trisacetylacetonate ($Cr(acac)_3$) were analyzed with a 4.8-s relaxation delay and inverse gated decoupling. The relaxation agent was added to decrease spin−lattice relaxation times and provide quantitative analyses. FTIR spectra were collected on a Nicolet Impact 400 FTIR spectrometer with liquid samples cast onto salt plates. Titrations to determine the concentration of carboxylic acid groups in the triblock polymers were conducted by dissolving the polymer (0.5 g) in 95 v/v % ethanol (25 mL) with 0.1 N KOH as titrant and phenolphthalein as an indicator. Each sample was titrated in triplicate to obtain an average concentration of carboxylic acids per gram of polymer. These values were converted into the concentrations of carboxylic acids per mole by taking the molecular weights of the polymers into consideration.

Characterization. Magnetite dispersion quality was investigated with a Philips 420T transmission electron microscope (TEM) and a JEOL 3000F field emission gun transmission electron microscope (FEGTEM) operating at 100 and 300 kV, respectively. Aqueous dispersions of the polymer−magnetite nanoparticle complexes were diluted to the appearance of a "weak tea", deposited on carbon-coated copper grids and allowed to air-dry. The presence of both iron and oxygen within the particles was confirmed by acquiring "elemental maps" using a Gatan Image Filter (GIF) attached to a JEOL 3000F FEGTEM. The particle size distributions were obtained by measuring the largest dimension of individual particles within a defined region of a micrograph, assuming the particles were single crystals. Areas containing aggregates were avoided in the analysis. The concentrations of Fe_3O_4 in the purified polymer−magnetite complexes were determined by elemental analyses. Elemental analysis was performed by Desert Analytics Laboratory (Tucson, AZ) by treating the samples with hot concentrated nitric acid followed by concentrated perchloric acid until complete dissolution was achieved. The sample solution was analyzed by inductively coupled plasma methods (ICP) to determine iron. Iron was calculated from sample response relative to standards and blanks.

The crystalline structure and particle sizes were investigated with powder X-ray diffractometry (XRD), selected area electron diffraction (SAED), and high-resolution electron microscopy (HREM). XRD studies of powder samples were performed with a Philips Electronics Instruments APD 3720 X-ray diffractometer. The X-ray diffraction patterns were taken from 10 to 80 (2θ value) using Cu Kα radiation. The SAED investigations were run on a JEOL 2000Fx II TEM at 80 kV. The HREM analyses were carried out using a JEOL 3000F FEGTEM operating at 300 kV equipped with a Gatan 694 multiscan camera and a Gatan Image Filter.

Magnetic properties of the polymer-coated magnetite nanoparticles were measured in the solid state at room temperature using a Standard 7300 Series Lakeshore vibrating sample magnetometer (VSM). The magnetic moment of each dried sample was measured over a range of applied fields from −8000 to +8000 Oe with a sensitivity of 0.1 emu. Magnetite mass specific magnetizations for each sample were calculated using the concentration of iron measured by ICP methods and assuming that all iron was in the form of magnetite.

III. Results and Discussion

Our primary objectives in this work were to develop methodologies for preparing dispersions (1) which were highly concentrated with discrete, polymer-coated magnetite nanoparticles and (2) which had the highest possible magnetite specific saturation magnetization. These nanoparticles were coated with biocompatible, hydrophilic stabilizers so that they could be dispersed in biological fluids. Dispersions of magnetite−polymer complexes were prepared by forming Fe_3O_4 crystals in aqueous base first and then coating these particles with the acidic copolymer dispersion stabilizers in interfacial reaction media.

Triblock copolymer stabilizers comprised of a central polyurethane "anchor block", which chemisorbed onto the magnetite surfaces, and hydrophilic "tail blocks" designed to extend out into water and provide dispersion stability were synthesized (Figure 1). The central anchor block lengths were systematically varied to contain averages of ≈3−10 carboxylic acid units to investigate the effects of multiple binding sites on the ability to produce dispersions which did not settle out even upon centrifugation. Previous studies have suggested that certain functional groups including carboxylic acids, phosphates, and sulfates can bind to magnetite.[28] Carboxylic acid groups have been reported to chemisorb onto magnetite surfaces through reaction with iron on the particle surfaces.[28,29]

Hydrophilic poly(ethylene oxide) oligomers are well-known to be biocompatible.[30,31] Additionally, living polymerizations of ethylene oxide can produce tail block lengths with controlled molecular weights, which enable the dispersions to be optimized. One important parameter was to determine the critical tail block length necessary to produce stable dispersions. The length of the stabilizing polymer chain must be sufficient to balance the magnetic attractions and the van der Waals attractive forces. However, excessively long polymer segments require space and, hence, lead to reduced magnetite concentrations in the polymer−nanoparticle complexes.

The molecular weights (M_n) of the monofunctional, poly(ethylene oxide) tail blocks investigated in this research ranged from 770 to 16 470 g/mol. Number average molecular weights were determined from ^{1}H NMR by ratioing the integrals of the methylene resonances centered at 3.65 ppm to the end group methoxy resonance at 3.38 ppm. Triblock polyurethane stabilizers incorporating these oligomers were synthesized in two-step procedures. The poly(ethylene oxide) was

(28) Cornell, R. M.; Schertmann, U. *The Iron Oxides: Structure, Properties, Reactions, Occurrence and Uses*; VCH Publishers: Weinheim, 1996.

(29) Rocchiccioli-Deltcheff, C.; Franck, R.; Cabuil, V.; Massart, R. *J. Chem. Res.* **1987**, *5*, 126−127.

(30) Otsuka, H.; Nagasaki, Y.; Kataoka, K. *Curr. Opin. Colloid Interface Sci.* **2001**, *6*, 3−10.

(31) Harris, J. M. *Poly(ethylene glycol) chemistry*; Plenum Press: New York, 1992.

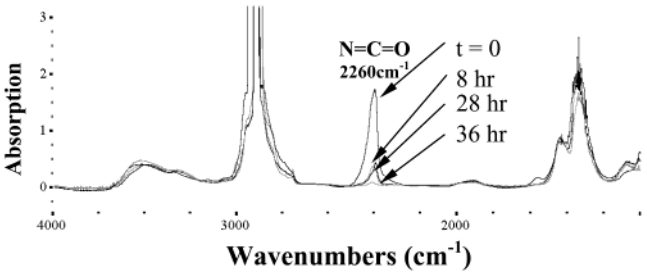

Figure 2. Disappearance of the isocyanate absorbance at 2260 cm^{-1} via FTIR during polyurethane synthesis of the carboxylic acid-containing triblock copolymers.

capped in the first step with an excess of the diisocyanate to ensure that the relatively high molecular weight component was quantitatively reacted into the block copolymer. It was important to have an excess of diisocyanate present during the first step to minimize coupling of monofunctional PEO oligomers. In the second step, the isocyanate species were reacted with the hydroxyl groups of bis(hydroxymethyl)propionic acid dissolved in a minimal amount of DMF to provide homogeneity.

Mild reaction conditions were utilized to minimize any reaction between the carboxylate group and isocyanate. Side reactions forming carbamates and CO_2 occurred with higher reaction temperatures and excessive catalyst. For example, reaction temperatures greater than 80 °C, DBTL catalyst concentrations above 800 ppm, or utilization of DMSO as a solvent all lead to loss of carboxylic acid functionality in the copolymers. Reaction completion was determined by the disappearance of the isocyanate (NCO) absorption peak via FTIR (Figure 2). The time required for complete isocyanate disappearance depended on the concentration of carboxylic acids incorporated into the polyurethane central segment of the polymer stabilizer. The synthesis of a triblock copolymer comprised of 1930 g/mol PEO tail blocks and ≈3 mol of bis(hydroxymethyl)propionic acid (≈3 carboxylic acid units) in the central polyurethane segment (connected by 4 mol of isophorone diisocyanate) required ≈36 h to achieve complete disappearance of the NCO peak (Figure 2).

The average degrees of polymerization of the polyurethane segments were varied from ≈3 to 10 to maximize the concentrations of magnetite in neutral dispersions. The average numbers of carboxylic acid groups per chain were determined by a combination of quantitative ^{1}H NMR (to quantify the molecular weights of the PEO tail blocks) and ^{13}C NMR (to determine the number of repeat units in the central polyurethane block). Titrations of carboxylic acid groups further confirmed the NMR data (Table 1). Number average molecular weights of the block copolymers were derived from ^{13}C NMR by ratioing the resonance integrals at 58 ppm due to the methoxy end groups on the PEO blocks to the peaks at 174.6 ppm (carboxylic acid carbonyl) and 18.5 ppm (methyl carbon on bis(hydroxymethyl)propionic acid) (Table 1 and Figure 3). Inverse gated decoupling and the use of the spin−spin relaxation agent, $Cr(acac)_3$, allowed for quantitative ^{13}C NMR analyses of the carboxylate groups (174.6 ppm). Near targeted values were obtained from the ^{13}C NMR analyses in $CDCl_3$, with the exception of significant deviation observed for the 4845PEO−9.9COOH−4845PEO stabilizer. It was reasoned that micelle structures in the chloroform solution, caused by the large number of acid groups in the central block, may have caused this deviation. When the sample was analyzed in d_6-DMSO, the measured concentration of carboxylate groups was similar to the targeted and titration values (Table 1). It was noteworthy that purified polymer stabilizers did not display peaks at 153.7 ppm in the ^{13}C NMR spectra, which confirmed the absence of residual isocyanate species.

Table 1. Concentrations of Carboxylic Acids/Mole Were Determined by Quantitative ^{13}C NMR, ^{1}H NMR, and Titrations[a]

targeted composition (PEO−COOH−PEO)	ave. no. of COOH/mol (^{13}C NMR)[b]	M_n[c] (g/mol)	ave. conc. of COOH/mol (titration)
770−**3**−770	2.6	2690	2.4 ± 0.06
1930−**3**−1930	3.1	5160	3.1 ± 0.04
1930−**5**−1930	2.4 (3.6)*	5340	3.6 ± 0.1
4845−**3**−4845	2.5	10 785	3.6 ± 0.1
4845−**5**−4845	4.7	11 540	6.7 ± 0.2
4845−**10**−4845	3.3 (9.9)*	13 410	10.2 ± 0.2

[a] The targeted numbers of carboxylic acids per mole are underlined in the composition column. [b] ^{13}C NMR samples were analyzed in $CDCl_3$ with the exception of the * samples, which were analyzed in d_6-DMSO. [c] Mn was based on the molecular weights of the end blocks obtained from ^{1}H NMR and the average numbers of carboxylate-containing units in the central block obtained from ^{13}C NMR. Where applicable, the ^{13}C data obtained in d_6-DMSO were utilized in the calculations.

Dispersions of the copolymer−magnetite nanoparticle complexes were prepared by first forming the Fe_3O_4 crystals in an aqueous base, and then these particles were coated with the acidic copolymer dispersion stabilizers in interfacial reaction media. Stoichiometric compositions ($Fe^{2+}/Fe^{3+} = 0.5$) of $FeCl_2$ and $FeCl_3$ were mixed and then condensed at room temperature under N_2 by reaction with hydroxide. These magnetite formation procedures were adapted from many previous studies.[32] All of the reactant solutions were carefully deoxygenated prior to reaction to avoid any oxidation of Fe^{2+} species. Black magnetite particles crystallized from the aqueous solutions almost immediately upon adding ammonium hydroxide to a pH of 9.5−10. This produced dispersions which would settle out if stirring was stopped, despite the fact that the pH was well above the isoelectric point of magnetite (6.8) and the particles were small. After base addition, the reactions were stirred at ambient temperature for 30 min to allow nucleation and crystal growth to occur.[28] The carboxylic acid-containing copolymer dispersion stabilizers, dissolved in dichloromethane, were added to the aqueous (negatively charged) magnetite dispersions and the carboxylic acids chemisorbed onto the anionic magnetite surfaces. The sequence of forming magnetite first, and then introducing the stabilizer, was chosen in an attempt to obtain the optimal crystalline structure. It had been suggested previously that if carboxylic acid functional groups were present during the crystallization of magnetite, the kinetics would be retarded and the crystallization mechanisms of iron oxide nanoparticle

(32) Cornell, R. M.; Schertmann, U. *Iron Oxides in the Laboratory; Preparation and Characterization.*; VCH: Weinheim, 1991.

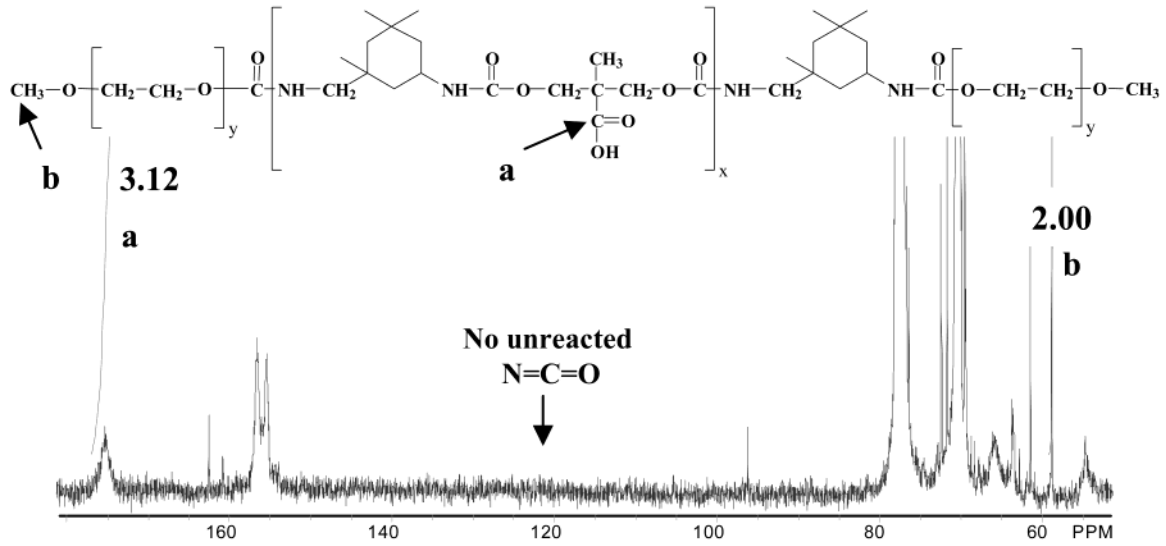

Figure 3. Quantitative ^{13}C NMR in $CDCl_3$ was utilized to assess the concentration of carboxylic acid carbons relative to end group carbons in the 1930PEO−3.1COOH−1930PEO triblock copolymer stabilizer.

formation would be adversely affected.[33,34] It should be noted that the central polyurethane block containing the carboxylic acids was not water-soluble and these block copolymers form aggregates in water. It is hypothesized that chemisorption of the acidic carboxylic acids onto the basic magnetite surfaces occurs at the dichloromethane−water interface. It is also noteworthy that when the aggregated polymer in water (without dichloromethane) was introduced into the reactions, chemisorption did not occur substantially (i.e., stable dispersions did not form). This could be attributed to inaccessibility of the carboxylic acids embedded in micellar structures and/or to formation of carboxylate anions in the basic aqueous medium. Anionic carboxylates would not be expected to adsorb substantially onto anionic magnetite surfaces due to charge repulsion.

After rapid agitation of the interfacial reaction mixtures for 30 min at a pH of ≈9, the dichloromethane was removed with a strong N_2 purge to transfer the polymer-coated magnetite nanoparticles completely into the water phase. If stirring was stopped at this stage, the particles would settle to the bottom of the flasks. However, when the pH of the reaction mixture was reduced to pH 6.5−7, stable dispersions formed. It is hypothesized that these dispersions were sterically stabilized with the hydrophilic PEO tail blocks since electrostatic interactions should not be sufficient at the isoelectric point of the magnetite (Figure 4).

The pH sensitivity of the dispersions was investigated by analyzing small aliquots from the solutions acquired at unit pH intervals from pH 10 to pH 2. These experiments showed that the dispersions became stable as the pH was reduced to between 8 and 7. The dispersions at pH > 8 were not stable and the magnetite nanoparticles settled within a few hours. At pH 8 the ferrofluids remained stable for approximately 1 week and then settled out of solution. However, dispersions

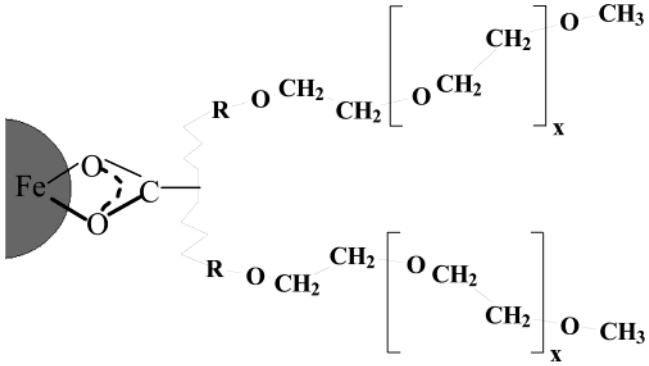

Figure 4. Central segment of the stabilizer anchors to the magnetite surface via the carboxylic acid groups while the hydrophilic tail blocks extend into water.

at pH 7 and down to pH 2 remained stable without sedimentation.

In these experiments the concentrations of polymer stabilizer were selected from calculations estimating the number of sites available for a carboxylate group to bind to an 8.8-nm-diameter spherical particle. The estimation of surface space required for binding one carboxylic acid, 0.16 nm^2, was borrowed from the low molecular weight surfactant literature.[35] For example, these calculations predicted that 1.76 g of the 1930PEO−3.6COOH−1930PEO polymer stabilizer would be needed to cover the surface of 0.857 g of 8.8-nm-diameter spherical magnetite particles (4.7×10^{17} Fe_3O_4 particles, 1520 sites/particle). Ideally, the polymer−magnetite complexes should be formed from the minimal polymer concentration necessary to create a stable dispersion. Minimizing the polymer coating will maximize the magnetophoretic mobility of the particles in a fluid. In applications where the magnetite nanoparticles are to be incorporated into microspheres, minimizing the polymer coating would also enable higher densities of particles to be incorporated into the microspheres.

(33) Krishnamurti, G. S. R.; Huang, P. M. *Clays Clay Miner.* **1991**, *39*, 28−34.

(34) Huang, P. M.; Wang, M. K. In *Advances in Geoecology*; Auerswald, K., Stanjek, H., Bigham, J. M., Eds.; International Development Centre: Ottawa, 1997; Vol. 30, pp 241−271.

(35) Wells, S. Preparation and Properties of Ultrafine Magnetic Particles. Ph.D. Thesis, University College of North Wales, Bangor, Wales, 1989.

Table 2. Comparisons of the Number of Magnetite Surface Binding Sites with the Number of Carboxylic Acid Binding Sites on the Stabilizers in Stable Magnetite-polymer Dispersions

polymer stabilizer[a]	concentration of magnetite charged to the dispersions (wt %)	concentration of magnetite stabilized (wt %)	theoretical no. of binding sites[b]	no. of COOH binding groups
770−2.6−770	50	45.4	3.1×10^{22}	3.2×10^{22}
1930−3.1−1930	50	37.4	2.6×10^{22}	2.3×10^{22}
1930−3.6−1930	35	23.0	1.6×10^{22}	3.1×10^{22}
4845−2.5−4845	46	30.2	2.1×10^{22}	1.0×10^{22}
4845−4.7−4845	30	22.8	1.6×10^{22}	1.9×10^{22}
4845−9.9−4845	30	7.8	5.4×10^{21}	4.1×10^{22}
16470−3−16470[c]	18	6.9	4.8×10^{21}	4.9×10^{21}

[a] The central number represents the data obtained from ^{13}C NMR for the number of carboxylic acid groups in the central polyurethane block of the stabilizer. [b] Calculated assuming spherical particles, the particle size distribution measured from TEM (Figure 7), and 0.16 nm^2 of surface area occupied per binding group. [c] The number of carboxylic acid groups was estimated from the amount charged to the copolymerization reaction.

Stable magnetite−copolymer dispersions were prepared with a series of polymers containing systematically varied block molecular weights (Table 2). Aqueous dispersions of these materials were dialyzed to remove any salts and then repeatedly centrifuged to remove any aggregates. The concentrations of magnetite in the magnetite−polymer complexes in these dispersions (after purification) were those described in column 3 of Table 2. The surface areas for the particular magnetite particle size distribution were calculated from the TEM data (see Figure 7) and yielded a surface area of 1.1×10^{20} nm^2/g. One can first observe that the comparisons between the number of binding sites and the number of binding groups available are remarkably similar. This suggests that the anchor blocks may be lying relatively flat against the particle surfaces, as opposed to forming large loops near the surface. It also suggests that multiple binding groups on a polymer chain were utilized for anchoring the chain to the particles. This may be important for achieving long-term dispersion stability. The one exception was that the copolymer having the longest central block (9.9 carboxylic acids per chain) did not bind efficiently under the conditions employed. Considerable additional work will be necessary to achieve a better understanding of the solution properties of these block copolymers and dispersions to resolve this issue. The polymer−magnetite complexes described in Table 2 with the shorter tail block lengths contained high concentrations of magnetite compared to previously reported polymer-coated iron oxide systems. For example, magnetite was stabilized with (1) PEO−PMA containing 5.5 wt % solids[21] and (2) dextran and PVA-based systems containing 0.56 and 7.7 w/w % iron, respectively.[22]

In terms of colloidal stability, a steric stabilizer creates repulsive forces to balance the magnetic attractive forces and the van der Waals attractive forces of the magnetic nanoparticles. Theory described by Rosensweig's modified Hamaker equation suggests that the stabilizer sheaths must be greater than 1−2 nm in a good solvent for the tail blocks to sterically stabilize 10-nm-diameter magnetite.[1] This expression considers the repulsive forces by converting a flat surface model into an integrated expression for two neighboring spheres. A sufficiently long stabilizer chain creates a potential energy barrier (≈25 kT) that is an order of magnitude greater than the thermal energy associated with each nanoparticle, so particle coalescence is minimized.[1]

Table 3. Theoretical Root-Mean Square End-to-End Distances of PEO Tail Block Segments of Polymer Stabilizers Calculated by Using the Characteristic Ratio for a Chain Attached by Its Terminus at an Interface

PEO block M_n (from ^1H NMR) (g/mol)	no. of backbone bonds (n)	$\langle r_0^2 \rangle^{1/2}$ (nm)
770	52	2.5
1930	131	3.9
4845	330	6.2
16470	1121	11.4

The end-to-end distance of an unperturbed polymer chain can be calculated by considering the characteristic ratio of a terminally attached chain (eq 1),[36]

$$C_n^{IF} = \frac{\langle r_0^2 \rangle}{nl^2} \quad (1)$$

where the characteristic ratio for a terminally attached chain is $C_n^{IF} = 4/3C_n^F$, C_n^F is the characteristic ratio for a free chain (4.0 for PEO), r_0^2 is the end-to-end distance, n is the number of bonds along the backbone, and l is the bond length (0.148 nm for PEO).[37] Calculation of the predicted end-to-end distance using the characteristic ratio is valid because the lowest M_n poly(ethylene oxide) tail block is sufficiently long to apply Gaussian statistics.[38] With this equation, the predicted end-to-end distance for a 770 g/mol poly(ethylene oxide) block is ≈2.5 nm. This suggests that our shortest poly(ethylene oxide) block should form a sufficiently thick polymer sheath to stabilize a 10-nm-diameter magnetite nanoparticle. The theoretical mean squared end-to-end distances for all of the PEO tail blocks investigated are provided in Table 3. However, it is important to note that these calculations are for polymers where the oligomer/particle attachment is at the terminus of the polymer chain. The volume available for the chains when they are attached by multiple sites along a central segment is more complicated and should differ somewhat due to ratios between tail and anchor block lengths.[37]

All of the copolymers described in Table 2 formed stable dispersions of 8.8 ± S.D. 2.7-nm-diameter mag-

(36) Napper, D. H. *Polymeric Stabilization of Colloidal Dispersions*; Academic Press: London, 1983.
(37) Russel, W. B.; Saville, D. A.; Schowalter, W. R. *Colloidal Dispersions*; Cambridge University Press: Cambridge, 1989.
(38) Flory, P. J. *Statistical Mechanics of Chain Molecules*; Hanser Publishers: Munich, 1989.

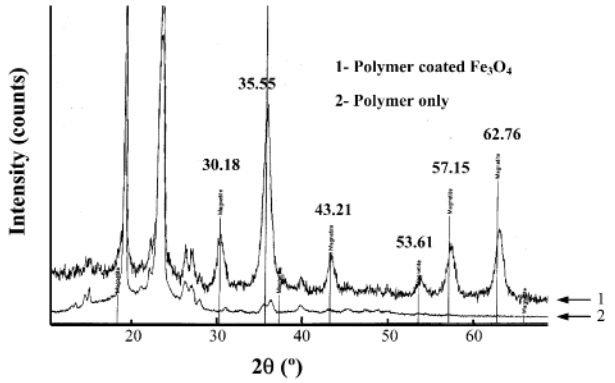

Figure 5. Overlay of powder XRD patterns, where spectrum 1 is Fe_3O_4 coated with a poly(ethylene oxide-*block*-urethane-*block*-ethylene oxide) polymer and spectrum 2 is the neat polymer.

netite in water and chlorinated solvents. Magnetite nanoparticles coated with thin layers of poly(ethylene oxide) may be sufficiently small to be eliminated through the human renal glomerular filtration system.[39] Thus, this size range may prove to be important for minimizing any toxicity considerations in biomedical applications.

The powder X-ray diffraction patterns of the polymer−nanomagnetite complexes displayed peak line positions and relative intensities consistent with the crystal structure of magnetite coated with the polymers (Figure 5). The XRD analyses also suggest the absence of other nonmagnetic, crystalline, iron oxide species; however, XRD cannot be used to completely refute the presence of maghemite due to similarities in the magnetite and maghemite diffraction patterns. It was important to note that the X-ray diffraction patterns confirmed that the ammonium chloride salt byproduct produced during magnetite formation had been removed by the dialysis purification procedure. Selected area electron diffraction patterns also suggest the magnetite crystal structure. The *d* spacings of 16 diffraction pattern rings were calculated and were within 2% error of literature values for the magnetite lattice.

The particle sizes and nature of purified, stable, aqueous dispersions of the magnetite−polymer complexes were studied with transmission electron microscopy. Dilute aqueous solutions of these complexes were placed onto copper TEM grids coated with a thin layer of carbon and allowed to air-dry. Magnetite nanoparticles coated with all the polymer stabilizer compositions appeared similar in the TEM micrographs (Figure 6a). "Elemental mapping" using a Gatan Image Filter attached to a FEGTEM indicated that all of the particles contained iron oxide. The conventional TEM image and corresponding iron element distribution map for a set of particles are shown in (a) and (b), respectively, of Figure 6. The large intensity variations between neighboring particles in Figure 6a are a result of diffraction contrast in the crystalline particles. The copolymer stabilizers (which were less electron dense) could not be clearly distinguished in the images.

The particle sizes were determined by measuring the lengths of over 100 particles within different regions of

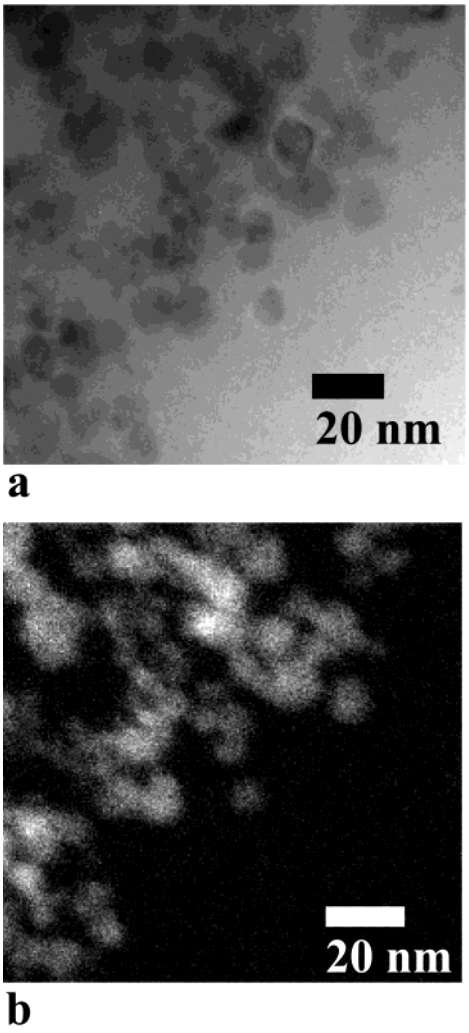

Figure 6. Transmission electron micrographs of magnetite nanoparticles stabilized with triblock stabilizers having poly(ethylene oxide) tail blocks and polyurethane anchor blocks with carboxylic acid groups on an amorphous carbon support film. In the conventional TEM image (a), the electron dense nanoparticles are visible against the lighter carbon support film. In the iron distribution image obtained via elemental mapping using a Gatan Image Filter (b), the bright regions indicate the presence of iron.

a given TEM grid containing a dispersion. The histogram of one such measured region (Figure 7) includes 184 particle measurements. The mean particle size distribution from two different regions of an identical dispersion were 8.8 ± S.D. 2.7 nm in diameter. As anticipated, all of the dispersions appeared to have similar particle size distributions.

High-resolution electron microscopy was used to verify the crystal structure and investigate the crystallinity of the nanoparticles. The particles were found to be single crystals ranging in size from ∼4 to 18 nm with a limited amount of aggregation (Figure 8a,b). Diffractograms (power spectra) of the individual particles (as shown in the inserts to the high-resolution images) demonstrated the single-crystal nature of the particles and were consistent with the magnetite structure.

The magnetite nanoparticles described in this paper were larger than many of the previously reported iron oxide systems which have been stabilized with polymers. Magnetite formed by the method reported herein

(39) Guyton, A. C.; Hall, J. E. In *Textbook of Medical Physiology*; W. B. Saunders Company: Philadelphia, 1996; pp 315−330.

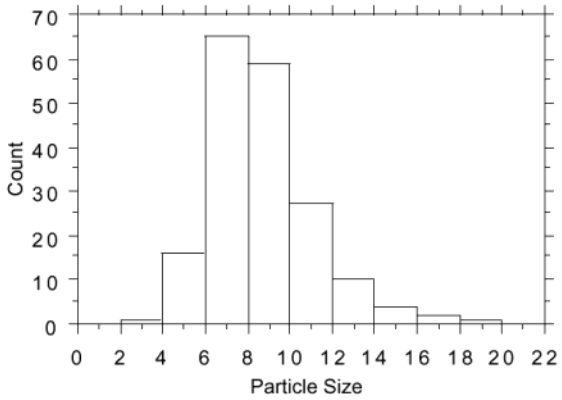

Figure 7. Particle size distribution of a dispersion of magnetite nanoparticles coated with a 770PEO−2.6COOH−770PEO triblock copolymer. The mean particle diameter = 8.7 ± S.D. 2.7 nm.

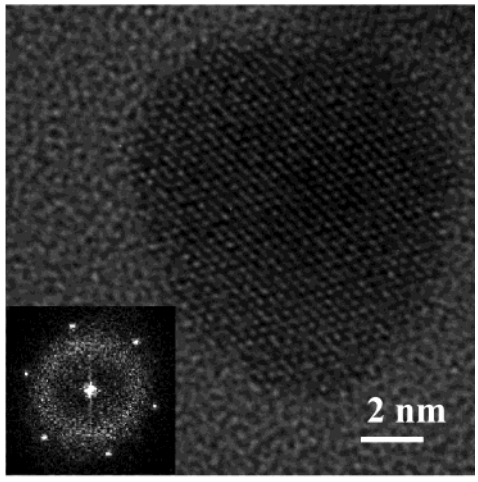

a

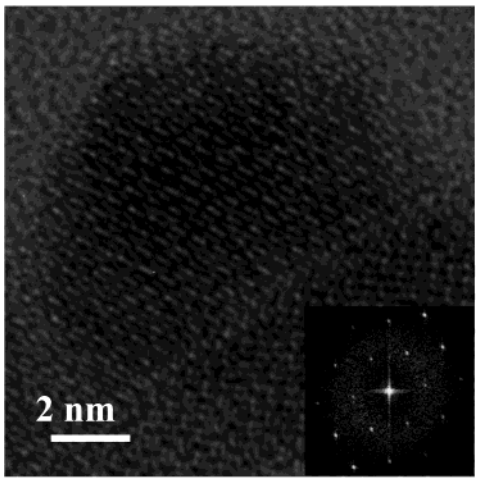

b

Figure 8. High-resolution TEM images of two magnetite nanoparticles. In (a), the ⟨111⟩ projection is observed, as confirmed by the presence of the six reflections in the diffractogram (insert) representing the 220 lattice spacing of 0.297 nm. The particle in (b) is viewed along the ⟨110⟩ projection, with the inner reflections in the diffractogram representing the 111 lattice spacing of 0.485 nm.

created 8.8 ± S.D. 2.7 nm diameter particles, while iron oxide particles formed in the presence of dextran and poly(vinyl alcohol) were 4.1 ± S.D. 0.8 and 5.8 ± S.D. 1.3 nm, respectively.[22] Moreover, the particles formed in the presence of dextran were clustered, and chains were reported in the dispersions formed in the presence of poly(vinyl alcohol).[22] The small size of those particles may have been due to the presence of the polymer during iron oxide formation. However, these polymer stabilizers did not contain carboxylic acid functional groups and therefore may have only superficially stabilized the nanoparticles.

Water-dispersible polymer stabilizers containing carboxylic acids, which have been previously reported, are poly(ethylene oxide)-*b*-poly(methacrylic acid) (PEO-*b*-PMA)[21] and a modified poly(ethylene oxide) containing two terminal carboxylate groups (DCPEG).[40] Both research groups reported the method of iron oxide formation by aqueous coprecipitation in the presence of the stabilizer. Magnetite nanoparticles prepared in the presence of PEO-*b*-PMA were ≈5 nm in diameter, with 5 nm of surfactant stabilizer, suggesting hydrodynamic radii of ≈15 nm. The DCPEG polymer stabilizer reported by Tamaura et al. was a modified poly(ethylene oxide) containing two terminal carboxylate groups.[40] The researchers reported that magnetite was formed in the presence of a 50 wt % solution of 2000 g/mol DCPEG. The large excess of DCPEG was used to promote coupling of lipase by reaction of the amine groups of the enzyme with the carboxyl groups of the polymer bound to the magnetite. Surprisingly, the size range of their particles was reported as 30−70 nm, but this may have been partially due to aggregates.[40] It is not clear why such large magnetite particles would form in the presence of the carboxylic acid-containing polymer stabilizer.

The magnetic properties of dried polymer-coated magnetite nanoparticles were investigated with vibrating sample magnetometry (VSM). Measurements of magnetite specific magnetization versus applied field yielded qualitatively similar results for all samples. An exemplary data set is shown in Figure 9. The magnetite nanoparticle−polymer complexes did not display magnetic remanence and initial slopes of the magnetization curves were steep, indicating superparamagnetic behavior with a high magnetic susceptibility. Magnetite specific saturation magnetizations are given in Table 4. The magnetization vs applied field curves were fitted with Langevin functions to model the superparamagnetic response of the particles. To obtain good fits to the data, it was necessary to include a linear magnetic susceptibility term representing an apparent paramagnetic component in the material. The number of particles per gram of magnetite deduced from the fitted Langevin function parameters enabled a characteristic particle volume to be determined by assuming that all of the iron was in the form of magnetite. Modeling the particles as spheres yielded diameters of approximately 12 nm for the characteristic volumes of each of the magnetite nanoparticle dispersions (mean 12.1 nm; S.D. 0.4 nm; $n = 5$). These magnetically determined values are consistent with the value of 12.3 nm for the diameter of the volume-weighted average volume of the particles calculated from the TEM measured particle size distribution. Experimental values for the saturation mag-

(40) Tamaura, Y.; Takahasi, K.; Kodera, Y.; Saito, Y.; Inada, Y. *Biotechnol. Lett.* **1986**, *8*, 877−880.

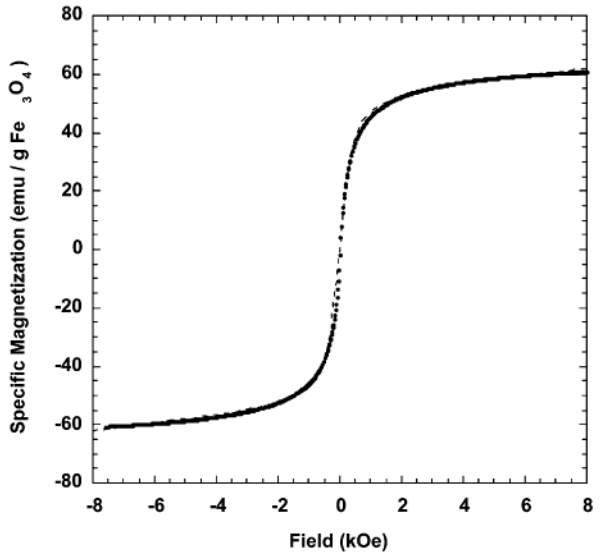

Figure 9. Magnetite specific magnetization vs applied field curve of a magnetite−triblock copolymer complex. The stabilizing triblock polymer was comprised of 4845 g/mol PEO tail blocks and a central polyurethane segment containing an average of 2.5 carboxylic acid units. The solid circles are the measured data while the dashed curve is a fit of a Langevin function and linear susceptibility to the data.

Table 4. Magnetic Properties of Magnetite Nanoparticles Stabilized with Poly(ethylene oxide-*block*-COOH-*block*-ethylene oxide) Triblock Stabilizers

polymer stabilizer	conc. of magnetite[a] (wt %)	saturation magnetic moment/ g of sample[b] (emu/g)	saturation magnetic moment/ g of Fe_3O_4 (emu/g)[b]
770−2.6−770	45.4	34	75
1930−3.1−1930	37.4	20	54
1930−3.6−1930	23.0	17	74
4845−2.5−4845	30.2	20	66
4845−4.7−4845	22.8	18	79
4845−9.9−4845	7.8	9	70
16470−3−16470[c]	6.9	5	67

[a] From iron elemental analyses. [b] Calculated from the magnetic moment of the sample in 8 kOe. [c] The number of carboxylic acid groups per chain was estimated from the concentration charged to the copolymerization reaction.

netization of magnetite nanoparticles reported for similar size iron oxide nanoparticles range from 30 to 60 emu/g, whereas bulk magnetite can theoretically be as high as 92 emu/g.[41,42] As a comparison, PEO-*b*-PMA-coated magnetite displayed a high saturation specific magnetization of ≈60 emu/g of Fe_3O_4, with a magnetite specific initial magnetic susceptibility of approximately 0.08 emu g^{-1} Oe^{-1}.[21] The initial magnetite specific magnetic susceptibility of the PEO-*b*-PMA-coated magnetite is low compared with an average value of 0.18 emu g^{-1} Oe^{-1} for the magnetite in our study.

There are several reasons why the saturation magnetization of magnetite nanoparticles may vary with different preparative methods. One theory offered by Davies et al. suggested that particles containing sufficient concentrations of functional groups allowed for spin-pinning of the iron oxide surfaces.[43] These results and others suggest that spin-pinning gives rise to a noncollinear spin structure, which is known to produce reduced magnetic moments on the particles.[43−45] These theories may help explain the low magnetic susceptibility of magnetite nanoparticles formed in the presence of poly(ethylene oxide)-*b*-poly(methacrylic acid) polymer stabilizers which contain significant concentrations of functional groups. The paramagnetic component in the magnetite dispersions in our study had contributions to the magnetic susceptibility ranging from 1.1×10^{-3} to 2.3×10^{-3} emu (g of Fe_3O_4)$^{-1}$ Oe^{-1}. The paramagnetic iron could possibly be related to iron atoms at the surface of the magnetite nanoparticles. However, further investigations will be required to confirm this hypothesis.

The lower saturation specific magnetization of nanoparticles compared to bulk material has been investigated by several researchers using a variety of techniques. The theories and experimental interpretations of these studies are in conflict and remain debatable. Some studies suggest that reduction of the observed magnetic moment as the particle size decreases depends largely on the crystalline magnetic anisotropy constant K for the material. The smaller K is, the less magnetization the particle can display.[42] Experimental analyses including microscopy, XRD, and magnetometry studies suggest that the reduced magnetization is due to surface characteristics of nanoparticles. Nevertheless, it seems that the effects of particle size in the nanolength scales are complex and alter relaxation processes and interparticle interactions.[41] Therefore, values of 60−70 emu/g of Fe_3O_4 may be approaching the limit in the specific magnetization for magnetite nanoparticles with diameter distribution ranges less than 20 nm.

IV. Conclusions

Triblock polymers were synthesized with controlled concentrations of carboxylic acid binding groups in central polyurethane segments and poly(ethylene oxide) end blocks. These polymers were demonstrated to be hydrophilic steric stabilizers for magnetite nanoparticle dispersions in water and chlorinated solvents. Magnetite nanoparticles were synthesized under strongly basic conditions, and then the polymers were adsorbed onto the particle surfaces in interfacial reactions. It is hypothesized that the acidic carboxylic acid groups adsorb onto the anionic magnetite surface at the dichloromethane−water interface. After adsorption of the polymer, it was necessary to neutralize (pH 6.5−7) the mixtures to maintain stable dispersions. These aqueous dispersions were stable at the physiological pH (7.4) and lower, suggesting that they will be stable in blood. The particle surface areas were calculated from TEM measurements of 100−184 particles in the images. After purification of the magnetite−polymer complexes, the number of carboxylic acid binding sites on the polymers were compared with the calculated number of magnetite surface sites (assuming 0.16 nm^2/site). These numbers

(41) Popplewell, J.; Sakhnini, L. *J. Magn. Magn. Mater.* **1995**, *149*, 72−78.
(42) Sato, T.; Iijima, T.; Sekin, M.; Inagaki, N. *J. Magn. Magn. Mater.* **1987**, *65*, 252−256.
(43) Davies, K. J.; Wells, S.; Charles, S. W. *J. Magn. Magn. Mater.* **1993**, *122*, 24−28.
(44) Coey, J. M. D. *Phys. Rev. Lett.* **1971**, *27*, 1140−1142.
(45) Morup, S. *J. Magn. Magn. Mater.* **1983**, *39*, 45−47.

corresponded reasonably well, suggesting that multiple binding sites on the polymers adsorb onto the magnetite.

The method of preparing stable magnetite dispersions may be generalized by altering the chemical compositions of the polymer tail segments. It may be possible to prepare triblock copolymers containing controlled concentrations of carboxylic acid groups in the central polyurethane segments with a variety of different hydroxyl-terminated polymer tail blocks, suggesting that this stabilization method could be generalized to serve diverse dispersion applications.

Transmission electron micrographs of stabilized magnetite showed Fe_3O_4 particles with a mean size of 8.8 $\pm$ S.D. 2.7 nm in diameter and a combination of isolated particles and small aggregates. Some aggregation may occur during the drying of the polymer−magnetite solvent on the TEM grid and it was difficult to estimate the initial level of aggregation in the polymer−magnetite matrix from these images. Therefore, ongoing work will include investigations of aqueous dispersion structures using small-angle X-ray scattering to give information on particle size distributions and clustering behavior in the aqueous state. The presence of iron and oxygen in the dispersed particles was confirmed by TEM elemental mapping. The crystal structure and single-crystal nature of the nanoparticles was verified via a combination of XRD, SAED, and HREM. The saturation magnetizations of these coated particles were as high as 34 emu/g. The shortest tail block length (770 Mn) was apparently sufficiently long to provide good steric stabilization in water, and shorter lengths will be analyzed in the future to maximize magnetite concentration. The saturation magnetization per gram of magnetite was approximately 65−70 emu/g for these 8.8-nm-diameter particles. This compares well with values reported by others for magnetite nanoparticles.[41,42] It will be important to optimize these dispersions to obtain higher concentrations of magnetite to maximize their response.

Acknowledgment. The authors would like to thank Prof. Phil Fraundorf and Sam Shuhan Lin of the University of Missouri at St. Louis for SAED analysis and Frank May of the University of Missouri at St. Louis for powder XRD analysis. Funding for this research was graciously provided by DARPA-AFOSR (Contract #F49620-01-1-0407) and by an NSF postdoctoral grant (NSF-IFRP Grant #INT-0207035).

CM020994N